Minireview

Ultrasound in ocular oncology: Technical advances, clinical applications, and limitations

Arya Kadakia[1], Junhang Zhang[2], Xincheng Yao[1,3], Qifa Zhou[2] and Michael J Heiferman[1]

[1]Department of Ophthalmology and Visual Sciences, Illinois Eye and Ear Infirmary, University of Illinois Chicago, Chicago, IL 60612, USA; [2]Department of Biomedical Engineering, Viterbi School of Engineering, University of Southern California, Los Angeles, CA 90089, USA; [3]Department of Biomedical Engineering, University of Illinois Chicago, Chicago, IL 60607, USA
Corresponding author: Michael J Heiferman. Email: mheif@uic.edu

Impact Statement

Ultrasound is an important imaging modality in ocular oncology with numerous clinical applications and some limitations. Ultrasound aids in accurate visualization of ocular tumors, which is important in diagnosis, monitoring, and treatment. This review article summarizes the use of ultrasound in ocular oncology and discusses its limitations.

Abstract

Due to its accessibility and ability for real-time image acquisition of ocular structures, ultrasound has high utility in the visualization of the eye, especially in ocular oncology. In this minireview, we summarize the technical rationale and applications of ultrasound modalities, A-scan, B-scan, high-frequency ultrasound biomicroscopy (UBM), and Doppler measurement. A-scan ultrasound uses a transducer of 7–11 MHz, making it useful for determining the echogenicity of ocular tumors (7–8 MHz) and measuring the axial length of the eye (10–11 MHz). B-scan ultrasound operates at 10–20 MHz, which can be used for measuring posterior ocular tumors while UBM operates at 40–100 MHz to evaluate anterior ocular structures. Doppler ultrasonography allows for the detection of tumor vascularization. While ultrasonography has numerous clinical applications due to its favorable penetration compared with optical coherence tomography, it is still limited by its relatively lower resolution. Ultrasound also requires an experienced sonographer due to the need for accurate probe localization to areas of interest.

Keywords: Ultrasound, sonography, A-scan, B-scan, ultrasound biomicroscopy, Doppler

***Experimental Biology and Medicine* 2023; 248: 371–379. DOI: 10.1177/15353702231169539**

Introduction

Reliable detection and quantitative assessment of ocular lesions are essential steps in the management of many vision- and life-threatening ocular diseases. The dilated fundus examination is complemented by numerous ancillary imaging modalities that are often required to arrive at an accurate diagnosis. Common optical imaging modalities include color fundus photography, fluorescein angiography, optical coherence tomography (OCT), and optical coherence tomography angiography (OCTA). Traditional color fundus photography provides valuable information for ocular disease diagnosis, lesion monitoring, and treatment response assessment.[1–4] However, traditional fundus photography produces an en face image, making volumetric quantification of ocular lesions difficult (Figure 1(a)).[5] OCT enables depth-resolved imaging at micrometer resolution, allowing accurate quantification of ocular lesions.[6–10] However, light-based OCT has limited penetration capability through the retinal pigment epithelium, choroid, and sclera where the light can be highly scattered and absorbed.[11] Enhanced depth imaging-OCT improves upon this limitation but cannot accurately evaluate thick lesions such as choroidal hemangiomas or retinal vasoproliferative tumors.[12–14] Moreover, ocular media opacity due to corneal pathology, dense cataract, vitreous cell, or hemorrhage; may limit the optical fundus imaging performance for reliable evaluation of ocular lesions.

Ultrasound imaging complements these limitations of optical imaging. Compared with light fundus photography, ultrasound imaging provides enhanced penetration capability, the ability to measure tissue acoustic impedance, and real-time image acquisition allowing for the kinetic evaluation of ocular structures.[15–17] Thus, there is utility of ultrasound in most subspecialties of ophthalmology including ocular oncology. In this minireview, we will summarize the technical rationales and applications of ultrasound modalities, such as A-scan, B-scan, high-frequency ultrasound

Copyright © 2023 by the Society for Experimental Biology and Medicine

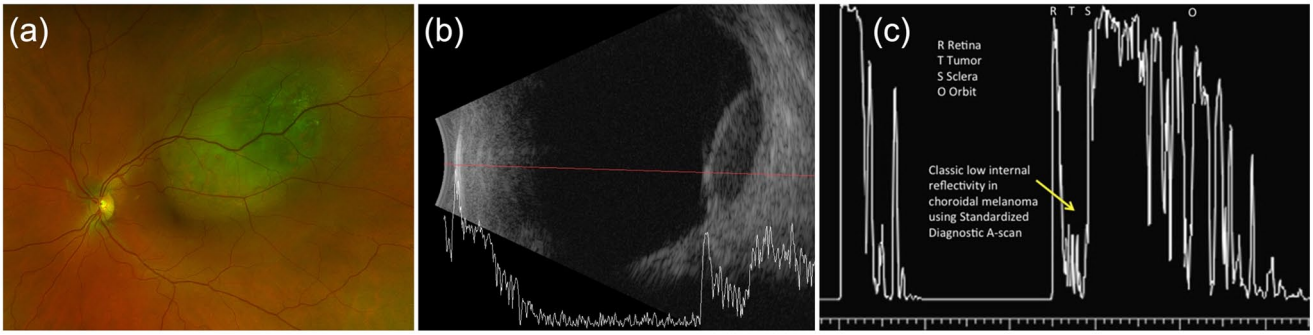

Figure 1. (a) Ultra-widefield light fundus photo of a uveal melanoma, (b) longitudinal B-scan ultrasound with overlayed cross-vector A-scan of a uveal melanoma and (c) standardized A-scan using 8-MHz probe of a uveal melanoma.
The arrow points to a low internal reflectivity from a small, pigmented lesion.
Source: Panel (c) is reprinted with permission from Kendall *et al.*[18]

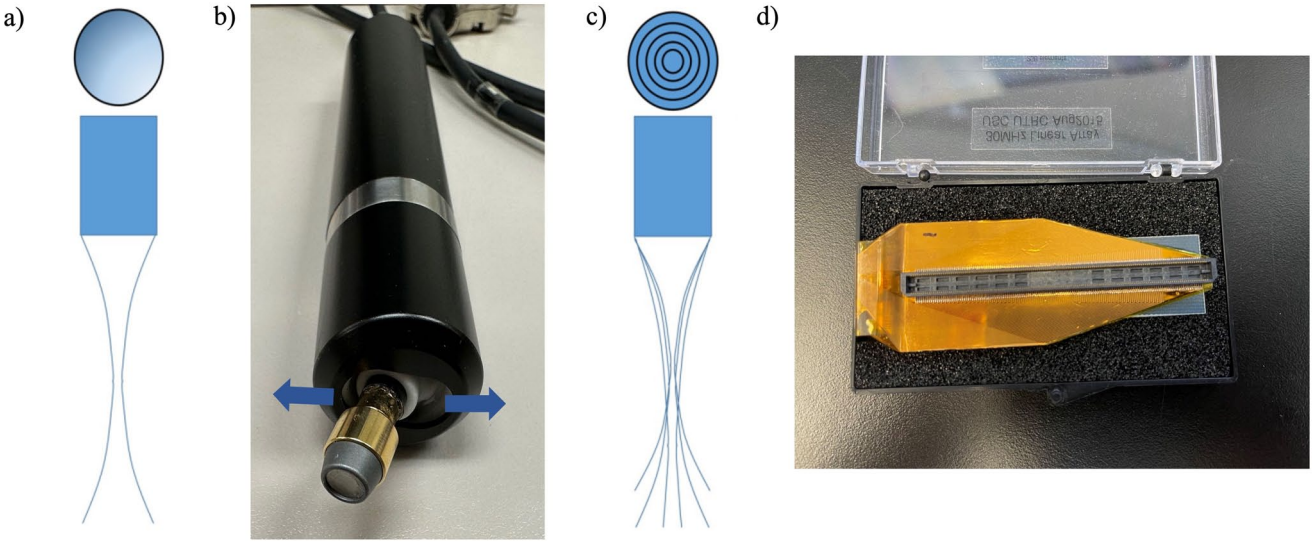

Figure 2. Ultrasound probes may be (a) single element, (b) UBM probe, (c) annular array, or (d) linear array.
Source: Panels (a) and (c) reprinted with permission from Silverman *et al.*[40]

biomicroscopy (UBM), and Doppler measurement. Current limitations and prospective developments in ocular oncology will also be discussed.

Ultrasound is a noninvasive imaging modality that uses high-frequency sound waves to create a detailed image of the eye. It is a widely accessible imaging modality with a low cost of use, minimal risk and does not require the use of ionizing radiation. More specifically, ultrasound has high utility in the visualization of the eye, and in the diagnosis and monitoring of ocular pathology due to the superficial location of the eye.[19] Ultrasound is a reliable modality for the diagnosis of many pathologies in ocular oncology, including the evaluation and monitoring of ocular tumors such as uveal melanoma.[15,20]

Using ultrasound in ophthalmology relies on transducers of different frequencies, depending on the resolution and depth of penetration required. Specifically, three types of ultrasound techniques are commonly used in ophthalmology: A-scans, B-scans, and UBM. A-scan is a one-dimensional scan of echo amplitude and therefore typically uses a single-element transducer (Figure 2). UBM also usually has a single high-frequency transducer, which is mechanically pivoted to obtain a two-dimensional image (Figure 2(b)).[15] However, in B-scan, arrays are used to gather a two-dimensional gray scale image. Arrays can be either linear or annular (Figure 2(c) and (d)). A linear array normally contains more than 32 elements and they are arranged linearly (Figure 2(a)). This also provides a faster scan rate than a single-element probe since scanning is controlled electronically rather than mechanically. Annular arrays have been recently introduced in commercial ophthalmic ultrasound systems and consist of a series of concentric transducer elements with fewer elements needed than in linear arrays, which facilitates the fabrication of high-frequency probes. However, the annular arrangement limits synthetic focusing to the beam axis, which requires mechanical scanning of the probe to obtain a B-scan. This reduces the scanning speed when compared with linear arrays, but it can provide attractive characteristics for imaging the eye because of the axial symmetry of the beam profile and large image depth.[15] Each modality can be advantageous for different uses due to their varying frequencies. The A-scan operates at a range of 7–11 MHz, the

B-scan at 10–20 MHz, and UBM at 40–100 MHz.[14,21] UBM and B-scan ultrasound can be used to measure the dimensions (axial and lateral) and volume of anterior and posterior ocular tumors, respectively (Figure 1(b)).[22] A-scan ultrasound can complement these modalities by measuring the tumor internal echogenicity and thickness (Figure 1(c)).

A-scan

The Amplitude-scan, or A-scan, is a one-dimensional scan of echo amplitude, operating at a frequency of 7–11 MHz for ophthalmic use. During an A-scan, the ultrasound transducer emits a single ultrasound pulse, and the distance to the reflecting tissues is calculated based on the time interval between pulse transmission and the speed of sound in tissue.[15] The echoes returning to the transducer are converted into amplitude spikes and the height of the spikes are proportional to the strength of the reflected echo signal. The A-scan mode is most commonly used for the measurement of axial length (AL) of the eye.[15,23] This makes A-scan particularly useful for planning cataract surgery, as axial length is needed for the determination of the power of the intraocular lens to be implanted into the eye. The status of the crystalline lens inside the eye and other variation in ocular media, such as a silicone oil-filled eye, changes the ultrasound signal and needs to be addressed to accurately determine the axial length. The reason for this variation is due to the difference of the speed of sound in different media with silicone oil being slower than in vitreous humor. When calculating the AL, the ultrasound machine only overestimates AL with a silicone oil-filled eye when the speed of sound in the oil (~1000 vs. 1540 m/s in vitreous) is not taken into account. This phenomenon was demonstrated by Murray *et al.*[24] when they measured the AL of seven phakic eyes with and without silicone oil in the vitreous cavity. Their results showed an apparent increase in AL induced by silicone oil compared with the control group without silicone oil due to the machine not correcting for the reduction in sound speed from 1532 m/s in vitreous to 987 m/s in silicone oil. Also, they proposed a correction factor to take into account the speed of sound in the silicone oil.

In the standardized echography technique, along with axial length measurements, A-scan is used to determine the echogenicity of the ocular tissues. The standardized A-scan is calibrated to a specific gain based on a tissue model to allow for accurate quantitative tissue evaluation (Figure 3(b)).[25] Alternatively, the cross-vector A-scan that can be overlayed to a B-scan is not calibrated and incorporates image processing that prevents a quantitative analysis. Vector A-scan is limited for tissue differentiation, since its amplification is logarithmic as it follows the B-scan. The logarithmic amplification method has a large dynamic range but low sensitivity, which makes it difficult to detect small differences in echo strength.[26] The A-scan has many clinical applications including diagnosing ocular tumors and differentiating between vitreous, retinal, and choroidal detachments.[27,28] Ocular tumors can be differentiated in part based on their internal echogenicity (Figure 1). In addition, ultrasound hollowness is a well-established risk factor for malignant transformation

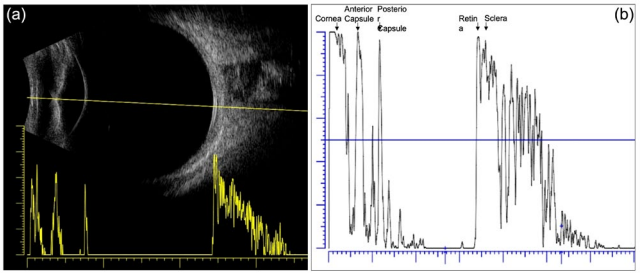

Figure 3. (a) Axial B-scan ultrasound with overlayed cross-vector A-scan of a normal eye and (b) standardized A-scan ultrasound of a normal eye. Source: Panel (b) from Medscape reference.

in patients with choroidal nevi.[29,30] A-scan is also used to evaluate for mimickers of ocular tumors including the reverberations seen with a dislocated intraocular lens and the high-amplitude peak of a metallic intraocular foreign body.

B-scan

The Brightness-scan, or B-scan, creates a two-dimensional, cross-sectional view of the eye using brightness intensity and amplitude of the echoes (Figure 3(a)).[15] For B-scan imaging, the ultrasound frequency ranges from 10 to 20 MHz, making it of higher resolution than the A-scan. This frequency can be used to visualize the posterior segment including the vitreous cavity, retina, choroid, sclera, and orbit. The posterior segment of the eye requires a longer focal length, which is achievable at the 10–20 MHz frequency range of B-scan. With more anterior tumors, there are physical limitations which prevent optimal probe positioning with B-scan and therefore, lower precision in measuring sloping lesions.[22,28] Instead, ultrasound with a shorter focal length optimizes visualization due to this limitation.

Due to its two-dimensional representation, B-scan allows for morphologic evaluation of ocular pathology, including determining anatomic location, shape, and borders of ocular tumors. For example, B-scan imaging can help in the detection of retinoblastoma by showing pathognomonic calcium deposits as highly reflective foci on the images.[31] It can also suggest optic nerve invasion from the retinoblastoma. To assist in the diagnosis and monitoring of uveal melanoma, a B-scan image can show a lenticular or mushroom-shaped mass, subretinal fluid, scleral erosions, or extraocular extension.[31] For choroidal nevi, the tumor size is associated with the risk for transformation to malignancy and patient prognosis. Clinical examination along with B-scan ultrasound can monitor the size and growth progression of choroidal nevi and indeterminate melanocytic choroidal tumors, which is essential for their management.[32]

Along with tumor measurement, ultrasound can contribute to the accurate localization to a lesion of interest, which is important in diseases that can develop multifocal lesions like choroidal metastasis and retinoblastoma.[33,34] Other tumor characteristics can be well demonstrated on ultrasound such as calcification, with a high amplitude and acoustic shadowing, which is seen in choroidal osteoma, optic disk drusen, and retinoblastoma. Another common use

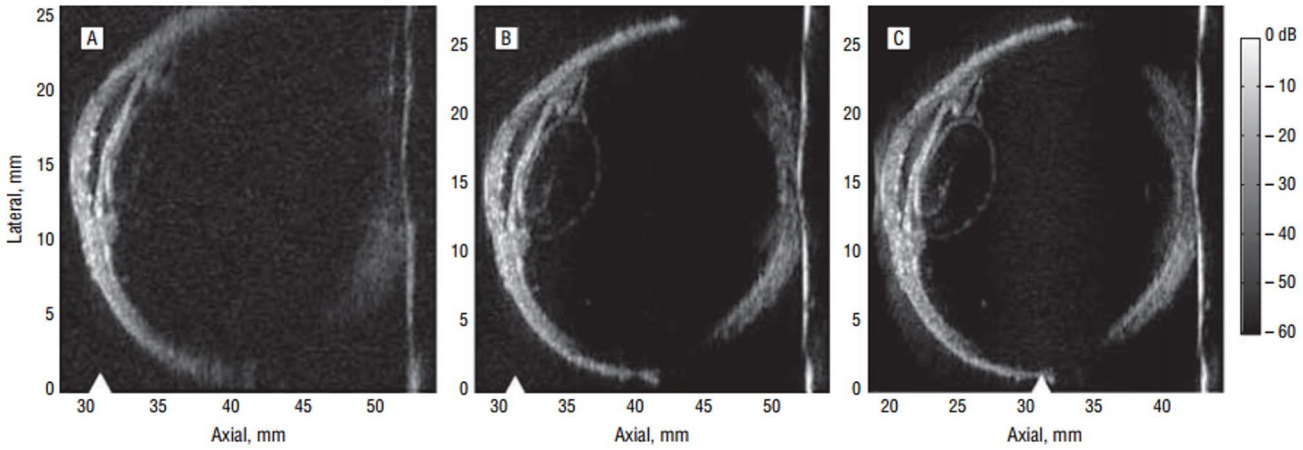

Figure 4. Whole eye images were acquired with the (A) 20-MHz annular array for cases of fixed focusing, (B) synthetic focusing with the 31-mm geometric focus (triangles) positioned just beyond the cornea and (C) with the geometric focus placed 1 cm deeper into the eye.
Source: Reprinted with permission from Silverman *et al.*[41]

of ultrasound is to assess the treatment response of a lesion. For uveal melanoma and retinoblastoma, treatment monitoring requires sequential ultrasound images to evaluate for local recurrence.[35]

Along with ocular tumor diagnosis and monitoring, B-scan is also used for confirmation of plaque brachytherapy placement in the radiation treatment of uveal melanoma and other ocular tumors. Accurate localization of the brachytherapy plaque to the tumor and minimizing plaque tilt away from the scleral wall ensures the appropriate treatment dose is subsequently delivered to the tumor.[36] Harbour *et al.*[37] found that 6 of 29 surgical cases (21%) required plaque repositioning after intraoperative ultrasound verification of plaque placement in patients with medium-size posterior uveal melanoma.[38] In a larger retrospective study, Tabandeh *et al.*[38] found that 28 of 117 surgical cases (24%) required repositioning due to incomplete coverage of the tumor margins, poor centration, or tilting of the plaque away from the sclera. In this way, B-scan ultrasound is used to diagnose, monitor progression, treat, and detect local recurrence of ocular tumors.

Within the frequency range of 10–20 MHz, the 10 and 20 MHz transducers each have their own advantages. Due to its higher resolution, 20 MHz B-scan can detect more details at the posterior pole. It can improve detection of lesion borders and the precision of measurements of posterior ocular tumors.[28] Coleman *et al.*[39] showed that 20-MHz scan provides more detail about tumor morphology when used to image small lesions and pigmented lesions compared with 10 MHz. They also showed the benefits of using 20 MHz for monitoring growth and structural changes in small tumors, even in the earliest stages.[40] According to Pineiro-Ces *et al.*,[40] the 20-MHz B-scan is favorable for detecting low internal echogenicity, which indicates tumor homogeneity and is an important risk factor for malignant transformation of choroidal nevi to uveal melanoma. They proposed that low internal echogenicity is easier to detect using the 20 MHz B-scan, because the echoes are attenuated more quickly with the 20 MHz than with 10 MHz when entering the tumor. However, these studies did not compare 10 or 20 MHz probes to unfocused 8-MHz A-scan probes for the detection of low internal echogenicity.

Conversely, 10-MHz B-scan better visualizes lower intensity reflectors such as the vitreous and has greater penetration to the orbit. Hewick *et al.*[21] demonstrated that 10-MHz compared with 20 MHz and proposed the use of 10 MHz in the evaluation of posterior vitreous detachments, hemorrhage, and inflammatory cell. They also demonstrated superior lateral and axial resolutions with the 20-MHz transducer at a distance of 10–24 mm, suggesting more accurate measurement of intraocular lesions. Since each transducer has its own advantages, a 10-MHz transducer may be used for initial screening including the orbit while a 20-MHz transducer may be used to evaluate intraocular lesions.[19] While a 10-MHz array can provide better image depth and a 20-MHz array can have higher resolution ophthalmic imaging, annular arrays, composed of a series of concentric rings, are capable of creating synthetically focused images without the complexity of phased arrays or linear arrays and with fewer elements. However, annular arrays must be mechanically scanned to create an image as single-element transducer. Silverman *et al.*[41] described a 20-MHz annular array probe that permits imaging of the full cross section of the eye with improved sensitivity and resolution in comparison with current single-element probes (Figure 4).

UBM

Ultrasound biomicroscopy, or UBM, has a frequency range of 40–100 MHz, thus providing better resolution of the anterior segment of the eye (Figure 5).[42] The mechanical transducer can be moved linearly or scanned in a sector fashion over a 5-mm image field within a coupling fluid-filled bath or water-filled bag. However, as the frequency increases, absorption does as well and signal penetration is limited to a depth of 3–6 mm. The signal penetration depends on the ultrasound attenuation coefficient of the tissue being imaged. As the frequency of the transducer increases, the attenuation coefficient increases, thus decreasing the penetration of the tissue. Structural tissues, like the sclera, have

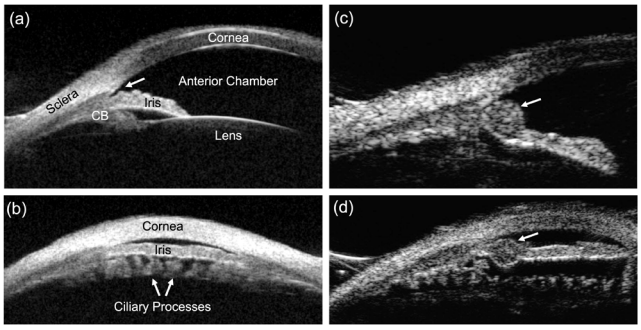

Figure 5. (a) Longitudinal ultrasound biomicroscopy of a normal eye (CB: ciliary body). (b) Transverse ultrasound biomicroscopy of a normal eye. (c) Longitudinal ultrasound biomicroscopy of an iris granuloma in a patient with sarcoidosis. (d) Transverse ultrasound biomicroscopy of the same iris granuloma.

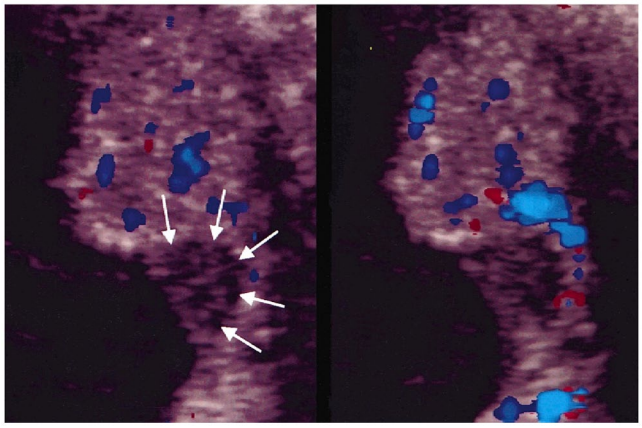

Figure 6. Doppler sonography, differentiating a tumor from subretinal fluid (effusion). The image on the left is the melanoma without contrast, while the image on the right shows the melanoma with contrast. The contrast-enhanced image shows detection of vascularization of the melanoma, which is absent in the subretinal fluid.
Source: Reprinted with permission from Lemke *et al*.[54]

high attenuation coefficients while the iris and cornea, more anterior structures, have lower attenuation coefficients.[42,43] The anterior structures also attenuate the acoustic signal, limiting the evaluation of posterior pathology.[15] However, the penetration of UBM images has less shadowing than anterior segment OCT (AS-OCT) but with lower resolution. Therefore, UBM complements AS-OCT allowing clinicians to better assess lesion thickness and intraocular invasion of nearby structures.[44,45]

UBM allows assessment of anterior segment structures, even if obscured by normal anatomic and pathologic relations, making it important for the evaluation of ocular surface, cornea, iris, ciliary body, anterior chamber angle, and lens.[46,47] UBM can be used clinically to detect tumors on the ocular surface and anterior segment, such as iris and ciliary body tumors as well as ocular surface squamous neoplasia and intraepithelial neoplasia (Figure 5).[48–50] Due to the reduction of posterior shadowing, UBM can also be a better tool to visualize posterior margins of lesions on the ocular surface, specifically of markedly elevated or darkly pigmented tumors compared with AS-OCT.[48,51]

Although UBM provides detailed images, it is limited by its penetration depth of around 3–6 mm depending on the frequency.[52] Its lower penetration restricts its use in the imaging of large tumors greater than 5–6 mm, where lower-frequency transducers have greater utility. UBM can be disadvantageous due to the greater skill needed to acquire and analyze the resulting images. UBM requires a coupling media, often distilled water, either in an immersion bath or water-filled bag, to obtain images requiring a more experienced user than ophthalmic B-scan.[45] The required direct contact to the eyeball surface limits the clinical use, preventing evaluation in patients with open globe trauma or active infection. The process of image acquisition can also be variable due to inconsistencies in alignments, and due to failure to control accommodation and room illumination.[42]

Doppler and contrast

Doppler ultrasound can be used to provide additional information in the diagnosis of ocular pathology. Conventional Doppler sonography uses the frequency shift of a tissue volume to measure flow conditions (velocity of flow, direction of flow) within vessels. Based on the frequency shift, false color can be added to images to illustrate the flow state of the vessel (Figure 6).[53,54] By convention, the motion toward the transducer is perceived as a higher frequency and is displayed in red and interpreted as arterial blood flow. Conversely, motion away from the transducer is lower frequency that is displayed as blue interpreted as venous flow. Power Doppler measures the strength, or power, of the signals returned by moving red blood cells. This makes it particularly useful for imaging slow or weak blood flow, such as in small blood vessels or in the presence of vascular stenosis. Power Doppler is more sensitive to flow, but does not capture velocity or flow direction.[55] Ultrasound contrasts can also be used to visualize the vasculature, specifically microbubble contrast agents due to their enhanced acoustic signal such as in the blood flow of a tumor.[56]

Due to their utility in visualizing vasculature, Doppler sonography and contrast have some utility in the diagnosis of ocular tumors. Walter *et al*.[57] conducted a study to understand the utility of color Doppler in the assessment of uveal melanoma, finding that color Doppler ultrasound can be used in conjunction with orbital magnetic resonance imaging to improve assessment of the tumor's vascularization. In a study by Iveković *et al*.,[58] the authors demonstrated that since vasculature growth varies between ocular tumors, color Doppler can be used to differentiate between patients with uveal melanoma, orbital hemangioma, and normal control subjects.

A study conducted by Kang *et al*.[22] assessed the use of a microbubble contrast agent to visualize vascularization of a uveal melanoma. They found that the microbubbles allow a better view of the microvascular blood flow in the tumor tissue potentially improving diagnostic efficacy of ultrasound using contrast. Lemke *et al*.[54] evaluated the use of a galactose microbubble contrast agent in patients with uveal melanoma. This study showed improved differentiation between uveal melanoma and associated subretinal fluid or hemorrhage with the use of a microbubble contrast. These authors also observed an improved detection of large orbital

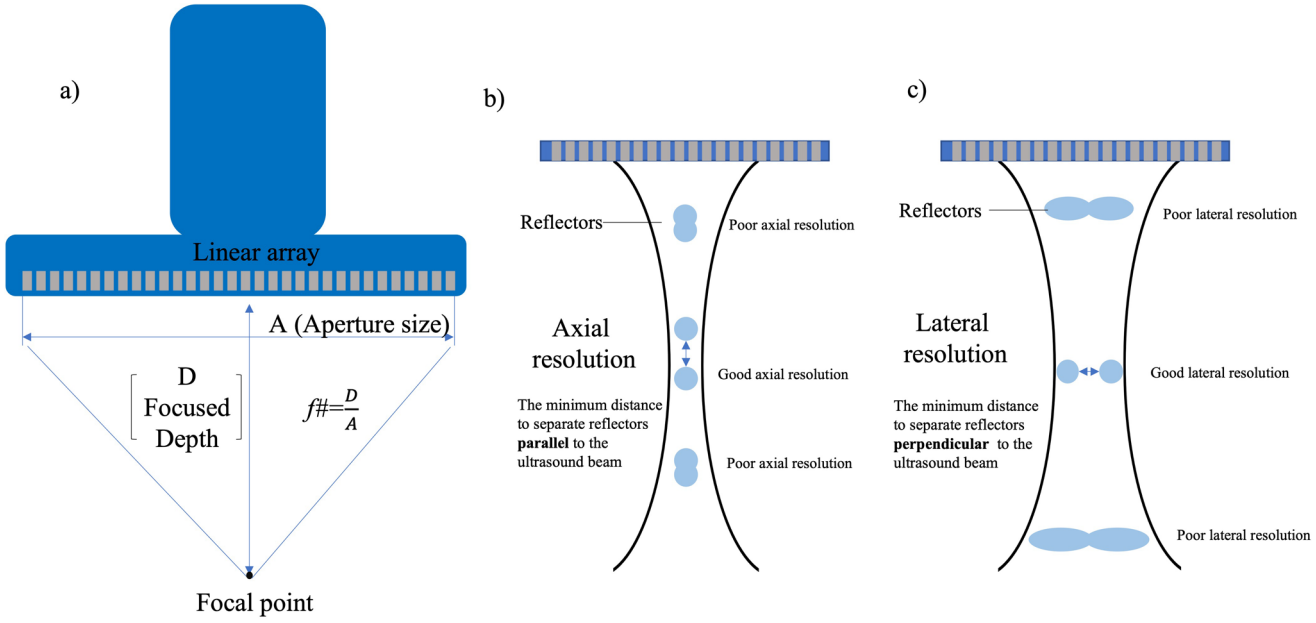

Figure 7. (a) Resolution calculation for linear array, (b) axial resolution, and (c) lateral resolution.

vessels with contrast while they found no improvement in the detection of tumor-associated small vessels.

Discussion

While ultrasound has many clinical applications, there are some limitations of its use in ocular oncology. One limitation is the relatively poor resolution of ultrasound compared with OCT by an order of magnitude.[59] The spatial resolution of ultrasound is determined by its axial and lateral resolutions (Figure 7). Axial resolution refers to the distance between two reflectors that can be distinguished when they are positioned parallel to the direction of the ultrasound beam. The axial resolution is determined by the spatial pulse length. Mathematically, it is equal to $\lambda n/2$, where λ is wavelength and n is the number of cycles per pulse.[60] Lateral resolution refers to the minimum distance that the system can distinguish of two reflectors arranged side by side, perpendicular to the beam. This characteristic is determined by both frequency and focal distance. Lateral resolution is calculated as $R(\text{lateral}) = \lambda * f\# = \lambda * D/A$, where D is the focal length, which is the distance between aperture and focal point, and A is the size of ultrasound aperture. Typically, a 10-MHz ultrasound transducer can have a resolution of 150 um in the axial direction and 450 um in the lateral direction, while for a 50 MHz UBM transducer, it can provide a resolution of 30 and 60 um in the axial and lateral directions, respectively.[59] Due to its better resolution, OCT is well suited for the measurement of tumor dimensions in cases of thin tumors.[39] The limited depth of penetration with OCT led to the development of enhanced depth-imaging, which is still limited in its ability to measure tumors thicker than 1.5 mm.[12–14,61] The increased sampling speeds of swept-source OCT have allowed for denser scan patterns and larger scan areas potentially improving the accurate measurement of the basal diameter of large tumors.[62,63] However, ultrasound remains the gold standard in the evaluation and monitoring of tumor thickness given its better penetration despite a lower resolution.

Due to its low cost and accessibility, the A-scan has provided useful applications for measuring the axial length of the eye prior to cataract surgery and in determining the echogenicity of ocular tissues to aid in the diagnosis of ocular tumors. However, the usability of the A-scan is somewhat challenging, due to difficulty in localizing the probe to the lesion of interest for novice users. For an A-scan to be accurately localized, it requires an experienced sonographer with the knowledge of ocular anatomy and ultrasound interpretation. The sonographer must also be able to consistently position the ultrasound probe, requiring repetitive practice. Accurate localization of the probe is also necessary when using B-scan imaging. To accurately measure the thickness and differentiate between a flat and elevated lesion, the lesion of interest must be positioned accurately by the sonographer. In general, ultrasound also has high inter-operator variability, requiring a skilled sonographer to correctly detect and evaluate ocular pathology.[64,65] Similarly, the experience of a sonographer can determine intra-examiner reliability for evaluating local recurrence of uveal melanoma. The apical height of a tumor is primarily used to report growth of the tumor, but local recurrence of a treated uveal melanoma can occur at any aspect rather than the apical tumor thickness.[66] To monitor for local recurrence, there must be consistency of ultrasound images to the area of interest, requiring an experienced sonographer.

Ultrasound also has limited ability when measuring axial length and the tumor size because when doing so, only the sonographically visible portion of the tumor can be measured. This means that ultrasound cannot measure truly flat pigmented portions of the tumor.[67] There are also inconsistencies when measuring the intraocular tumor largest basal diameter by a single-chord length using B-scan ultrasound for a uveal melanoma.[63] The lesions tend to be undersized

with this single-chord length technique. Since there is no gold standard for tumor basal diameter measurement, and instead these tumors must be monitored by experienced clinicians monitor the clinical examination along with other available imaging modalities.[63]

In the radiation treatment of patients with uveal melanoma, transillumination and B-scan can each be used to confirm plaque brachytherapy location at the time of insertion and removal. However, both transillumination and ultrasound imaging have limitations in doing so. Bayat *et al*.[68] identified multiple errors associated with the accurate localization of plaques to tumors using ultrasound. The lens inside the eye causes signal attenuation and refraction leading to artifactually opaque areas and image distortion of the plaque edge nearest to the lens. The ultrasound image can also have a ghost image due to the total internal reflection of the lens. These ultrasound artifacts are more significant for imaging tumors anterior to the equator, which is complemented by the transillumination technique for tumor localization. Transillumination of the semi-transparent eye to visualize the tumor borders which is also limited in large tumors due to shadowing by the tumor on the sclera. Knowledge of these artifacts and subsequent ultrasound transducer position adjustment are useful in optimizing plaque localization.

Conclusions

In conclusion, multiple ultrasound modalities including A-scan, B-scan, and UBM have been well established for use in ocular oncology. Ultrasound provides valuable information for visualizing anterior tumors with high-frequency UBM and posterior tumors with B-scan ultrasound. A-scan ultrasound is used to measure the tumor internal echogenicity and its thickness. Doppler and contrast have been used to detect tumor vascularization. Ultrasound has limitations due to inter-operator variability, lower resolution compared with OCT, and steep learning curve for the accurate localization of the probe to an area of interest. Current and further developments for ultrasound involve extended-field acquisitions, unfocused ultrasound using linear array-based technology, and advances in the signal transmission and reception process.[15,69] These advances have the potential to increase the utility of ultrasound in ocular oncology.

AUTHORS' CONTRIBUTIONS

A.K. drafted the manuscript. J.Z., X.Y., Q.Z., and M.H. contributed to the manuscript and figure preparation.

DECLARATION OF CONFLICTING INTERESTS

The author(s) declared no potential conflicts of interest with respect to the research, authorship, and/or publication of this article.

FUNDING

The author(s) received no financial support for the research, authorship, and/or publication of this article.

ORCID IDS

Arya Kadakia https://orcid.org/0000-0002-3377-9116
Xincheng Yao https://orcid.org/0000-0002-0356-3242
Michael J Heiferman https://orcid.org/0000-0003-3456-0164

REFERENCES

1. Ducrey NM, Delori FC, Gragoudas ES. Monochromatic ophthalmoscopy and fundus photography. II. The pathological fundus. *Arch Ophthalmol* 1979;**97**:288–93
2. Han YS, Pathipati M, Pan C, Leung LS, Blumenkranz MS, Myung D, Toy BC. Comparison of telemedicine screening of diabetic retinopathy by mydriatic smartphone-based vs nonmydriatic tabletop camera-based fundus imaging. *J Vitreoretin Dis* 2021;**5**:199–207
3. Bursztyn L, Woodward MA, Cornblath WT, Grabe HM, Trobe JD, Niziol L, De Lott LB. Accuracy and reliability of a handheld, nonmydriatic fundus camera for the remote detection of optic disc edema. *Telemed J E Health* 2018;**24**:344–50
4. McGrory S, Cameron JR, Pellegrini E, Warren C, Doubal FN, Deary IJ, Dhillon B, Wardlaw JM, Trucco E, MacGillivray TJ. The application of retinal fundus camera imaging in dementia: a systematic review. *Alzheimers Dement* 2016;**6**:91–107
5. Flower RW, Csaky KG, Murphy RP. Disparity between fundus camera and scanning laser ophthalmoscope indocyanine green imaging of retinal pigment epithelium detachments. *Retina* 1998;**18**:260–8
6. Coppola M, Marchese A, Cicinelli MV, Rabiolo A, Giuffrè C, Gomarasca S, Querques G, Bandello F. Macular optical coherence tomography findings after vitreoretinal surgery for rhegmatogenous retinal detachment. *Eur J Ophthalmol* 2020;**30**:805–16
7. Kim JY, Park SP. Macular hole formation and spontaneous closure after vitrectomy for rhegmatogenous retinal detachment documented by spectral-domain optical coherence tomography: case report and literature review. *Indian J Ophthalmol* 2015;**63**:791–3
8. Ghadri JR, Gaehwiler R, Jaguszewski M, Sudano I, Osipova J, Schoenenberger-Berzins R, Erne P, Lüscher TF, Templin C. Impact of local vascular lesions assessed with optical coherence tomography and ablation points on blood pressure reduction after renal denervation. *Swiss Med Wkly* 2015;**145**:w14102
9. Scalone G, Niccoli G, Refaat H, Vergallo R, Porto I, Leone AM, Burzotta F, D'Amario D, Liuzzo G, Fracassi F, Trani C, Crea F. Not all plaque ruptures are born equal: an optical coherence tomography study. *Eur Heart J Cardiovasc Imaging* 2017;**18**:1271–7
10. Shields CL, Manalac J, Das C, Saktanasate J, Shields JA. Review of spectral domain enhanced depth imaging optical coherence tomography of tumors of the choroid. *Indian J Ophthalmol* 2015;**63**:117–21
11. Mrejen S, Fung AT, Silverman RH, Kendall C, Freund KB. Potential pitfalls in measuring the thickness of small choroidal melanocytic tumors with ultrasonography. *Retina* 2013;**33**:1293–9
12. Spaide RF, Koizumi H, Pozzoni MC. Enhanced depth imaging spectral-domain optical coherence tomography. *Am J Ophthalmol* 2008;**146**:496–500. Erratum in: *Am J Ophthalmol* 2009;148:325. Pozonni, Maria C [corrected to Pozzoni, Maria C].
13. Shields CL, Kaliki S, Rojanaporn D, Ferenczy SR, Shields JA. Enhanced depth imaging optical coherence tomography of small choroidal melanoma: comparison with choroidal nevus. *Arch Ophthalmol* 2012; **130**:850–6
14. Kim RS, Jain RR, Brown DM, Bretana ME, Kegley EN, Singer MA, Aragon AV, Schefler AC. Elevated choroidal thickness and central serous chorioretinopathy in the fellow eyes of patients with circumscribed choroidal hemangioma. *Ocul Oncol Pathol* 2018;**4**:375–80
15. Silverman RH. Focused ultrasound in ophthalmology. *Clin Ophthalmol* 2016;**10**:1865–75
16. Hoffmann B, Schafer JM, Dietrich CF. Emergency ocular ultrasound—common traumatic and non-traumatic emergencies diagnosed with bedside ultrasound. *Ultraschall Med* 2020;**41**:618–645.
17. Alexander JL, Wei L, Palmer J, Darras A, Levin MR, Berry JL, Ludeman E. A systematic review of ultrasound biomicroscopy use in pediatric ophthalmology. *Eye* 2021;**35**:265–76

18. Kendall CJ, Prager, TC, Cheng H, Gombos D, Tang RA, Schiffman, JS. Diagnostic ophthalmic ultrasound for radiologists. *Neuroimaging Clin N Am* 2015;**25**:327–365
19. Nagaraju RM, Gurushankar G, Kadakola B. Efficacy of high frequency ultrasound in localization and characterization of orbital lesions. *J Clin Diagn Res* 2015;**9**:TC01–6
20. Solnik M, Paduszyńska N, Czarnecka AM, Synoradzki KJ, Yousef YA, Chorągiewicz T, Rejdak R, Toro MD, Zweifel S, Dyndor K, Fiedorowicz M. Imaging of uveal melanoma-current standard and methods in development. *Cancers* 2022;**14**:3147
21. Hewick SA, Fairhead AC, Culy JC, Atta HR. A comparison of 10 MHz and 20 MHz ultrasound probes in imaging the eye and orbit. *Br J Ophthalmol* 2004;**88**:551–5
22. Kang SJ, Zhang Q, Patel SR, Berezovsky D, Yang H, Wang Y, Grossniklaus HE. In vivo high-frequency contrast-enhanced ultrasonography of choroidal melanoma in rabbits: imaging features and histopathologic correlations. *Br J Ophthalmol* 2013;**97**:929–33
23. Bencic G, Vatavuk Z, Marotti M, Loncar VL, Petric I, Andrijevic-Derk B, Skunca J, Mandic Z. Comparison of A-scan and MRI for the measurement of axial length in silicone oil-filled eyes. *Br J Ophthalmol* 2009; **93**:502–5
24. Murray D, Potamitis T, Good P, Kirkby GR, Benson MT. Biometry of the silicone oil-filled eye. *Eye* 1999;**13**:319–24
25. Byrne SF. Standardized echography of the eye and orbit. *Neuroradiology* 1986;**28**:618–40
26. Aung T, Chopdar A. *Multimodal retinal imaging*. India: JP Medical Publishers, 2014
27. Singh N, Fonkeu Y, Lorek BH, Singh AD. Diagnostic A-scan of choroidal tumors: comparison of quantified parameters. *Ocul Oncol Pathol* 2019;**5**:358–68
28. Kook D, Kreutzer TC, Wolf A, Haritoglou C. Variability of standardized echographic ultrasound using 10 mHz and high-resolution 20 mHz B scan in measuring intraocular melanoma. *Clin Ophthalmol* 2011;**5**:477–82
29. Shields CL, Shields JA, Kiratli H, De Potter P, Cater JR. Risk factors for growth and metastasis of small choroidal melanocytic lesions. *Ophthalmology* 1995;**102**:1351–61
30. Factors predictive of growth and treatment of small choroidal melanoma: COMS Report No. 5. The Collaborative Ocular Melanoma Study Group. *Arch Ophthalmol* 1997;**115**: 1537–44
31. Aironi VD, Gandage SG. Pictorial essay: B-scan ultrasonography in ocular abnormalities. *Indian J Radiol Imaging* 2009;**19**:109–15
32. Shields CL, Furuta M, Berman EL, Zahler JD, Hoberman DM, Dinh DH, Mashayekhi A, Shields JA. Choroidal nevus transformation into melanoma: analysis of 2514 consecutive cases. *Arch Ophthalmol* 2009;**127**:981–7
33. Blasi MA, Maceroni M, Caputo CG, Sammarco MG, Scupola A, Lenkowicz J, Schinzari G, Rossi E, Pagliara MM. Clinical and ultrasonographic features of choroidal metastases based on primary cancer site: long-term experience in a single center. *PLoS ONE* 2021;**16**: e0249210
34. Finger PT, Khoobehi A, Ponce-Contreras MR, Rocca DD, Garcia JP Jr. Three dimensional ultrasound of retinoblastoma: initial experience. *Br J Ophthalmol* 2002;**86**:1136–8
35. Ophthalmic Oncology Task Force. Local recurrence significantly increases the risk of metastatic uveal melanoma. *Ophthalmology* 2016; **123**:86–91
36. Pavlin CJ, Japp B, Simpson ER, McGowan HD, Fitzpatrick PJ. Ultrasound determination of the relationship of radioactive plaques to the base of choroidal melanomas. *Ophthalmology* 1989;**96**:538–42
37. Harbour JW, Murray TG, Byrne SF, Hughes JR, Gendron EK, Ehlies FJ, Markoe AM. Intraoperative echographic localization of iodine 125 episcleral radioactive plaques for posterior uveal melanoma. *Retina* 1996;**16**:129–34
38. Tabandeh H, Chaudhry NA, Murbeam TG, Ehlies F, Hughes R, Scott IU, Markoe AM. Intraoperative echographic localization of iodine-125 episcleral plaque for brachytherapy of choroidal melanoma. *Am J Ophthalmol* 2000;**129**:199–204
39. Coleman DJ, Silverman RH, Chabi A, Rondeau MJ, Shung KK, Cannata J, Lincoff H. High-resolution ultrasonic imaging of the posterior segment. *Ophthalmology* 2004;**111**:1344–51
40. Piñeiro-Ces A, Rodríguez Alvarez MJ, Santiago M, Bande M, Pardo M, Capeáns C, Blanco MJ. Detecting ultrasonographic hollowness in small choroidal melanocytic tumors using 10 MHz and 20 MHz ultrasonography: a comparative study. *Graefes Arch Clin Exp Ophthalmol* 2014;**252**:2005–11
41. Silverman RH, Ketterling JA, Mamou J, Coleman DJ. Improved high-resolution ultrasonic imaging of the eye. *Arch Ophthalmol* 2008;**126**:94–7
42. Foster FS, Pavlin CJ, Harasiewicz KA, Christopher DA, Turnbull DH. Advances in ultrasound biomicroscopy. *Ultrasound Med Biol* 2000; **26**:1–27
43. Foster FS, Lockwood GR, Ryan LK, Harasiewicz KA, Berube L, Rauth AM. Principles and applications of ultrasound backscatter microscopy. *IEEE Trans Ultrason Ferroelectr Freq Control* 1993;**40**:608–17
44. Kuzmanović Elabjer B, Bušić M, Bišćan Tvrdi A, Miletić D, Bosnar D, Bjeloš M. Ultrasound reliability in detection of retinal tear in acute symptomatic posterior vitreous detachment with vitreous hemorrhage. *Int J Ophthalmol* 2017;**10**:1922–4
45. Venkateswaran N, Sripawadkul W, Karp CL. The role of imaging technologies for ocular surface tumors. *Curr Opin Ophthalmol* 2021;**32**: 369–78
46. He M, Wang D, Jiang Y. Overview of ultrasound biomicroscopy. *J Curr Glaucoma Pract* 2012;**6**:25–53
47. Bianciotto C, Shields CL, Guzman JM, Romanelli-Gobbi M, Mazzuca D Jr, Green WR, Shields JA. Assessment of anterior segment tumors with ultrasound biomicroscopy versus anterior segment optical coherence tomography in 200 cases. *Ophthalmology* 2011;**118**:1297–302
48. Konopińska J, Lisowski Ł, Wasiluk E, Mariak Z, Obuchowska I. The effectiveness of ultrasound biomicroscopic and anterior segment optical coherence tomography in the assessment of anterior segment tumors: long-term follow-up. *J Ophthalmol* 2020;**2020**:9053737
49. Neupane R, Gaudana R, Boddu SHS. Imaging techniques in the diagnosis and management of ocular tumors: prospects and challenges. *AAPS J* 2018;**20**:97
50. Thomas BJ, Galor A, Nanji AA, El Sayyad F, Wang J, Dubovy SR, Joag MG, Karp CL. Ultra high-resolution anterior segment optical coherence tomography in the diagnosis and management of ocular surface squamous neoplasia. *Ocul Surf* 2014;**12**:46–58
51. Vizvári E, Skribek Á, Polgár N, Vörös A, Sziklai P, Tóth-Molnár E. Conjunctival melanocytic naevus: diagnostic value of anterior segment optical coherence tomography and ultrasound biomicroscopy. *PLoS ONE* 2018;**13**:e0192908
52. Ghassemi F. Ultrasonography (B-scan) and ultrasound biomicroscopy (UBM). In: Mohammadpour M (eds) *Diagnostics in ocular imaging*. Cham: Springer, 2021
53. Martinoli C, Derchi LE, Rizzatto G, Solbiati L. Power Doppler sonography: general principles, clinical applications, and future prospects. *Eur Radiol* 1998;**8**:1224–35
54. Lemke AJ, Hosten N, Richter M, Bechrakis NE, Foerster P, Puls R, Gutberlet M, Felix R. Contrast-enhanced color Doppler sonography of uveal melanomas. *J Clin Ultrasound* 2001;**29**:205–11
55. Modrzejewska M. Guidelines for ultrasound examination in ophthalmology. *J Ultrason* 2019;**19**:128–36
56. Ferrara K, Pollard R, Borden M. Ultrasound microbubble contrast agents: fundamentals and application to gene and drug delivery. *Annu Rev Biomed Eng* 2007;**9**:415–47
57. Walter U, Niendorf T, Graessl A, Rieger J, Krüger PC, Langner S, Guthoff RF, Stachs O. Ultrahigh field magnetic resonance and colour Doppler real-time fusion imaging of the orbit—a hybrid tool for assessment of choroidal melanoma. *Eur Radiol* 2014;**24**:1112–7
58. Iveković R, Lovrencić-Huzjan A, Mandić Z, Talan-Hranilović J. Color Doppler flow imaging of ocular tumors. *Croat Med J* 2000;**41**:72–5
59. Silverman RH. High—resolution ultrasound imaging of the eye—a review. *Clin Exp Ophthalmol* 2009;**37**:54–67
60. Alexander Ng, Justiaan S. Resolution in ultrasound imaging. *Contin Educ Anaesth Crit Care Pain* 2011;**11**:186–92

61. Shah SU, Kaliki S, Shields CL, Ferenczy SR, Harmon SA, Shields JA. Enhanced depth imaging optical coherence tomography of choroidal nevus in 104 cases. *Ophthalmology* 2012;**119**:1066–72
62. Miller AR, Roisman L, Zhang Q, Zheng F, Rafael de Oliveira Dias J, Yehoshua Z, Schaal KB, Feuer W, Gregori G, Chu Z, Chen CL, Kubach S, An L, Stetson PF, Durbin MK, Wang RK, Rosenfeld PJ. Comparison between spectral-domain and swept-source optical coherence tomography angiographic imaging of choroidal neovascularization. *Invest Ophthalmol Vis Sci* 2017;**58**:1499–505. Erratum in: *Invest Ophthalmol Vis Sci* 2017;58:2166
63. Potsaid B, Baumann B, Huang D, Barry S, Cable AE, Schuman JS, Duker JS, Fujimoto JG. Ultrahigh speed 1050nm swept source/Fourier domain OCT retinal and anterior segment imaging at 100,000 to 400,000 axial scans per second. *Opt Express* 2010;**18**:20029–48
64. Tello C, Liebmann J, Potash SD, Cohen H, Ritch R. Measurement of ultrasound biomicroscopy images: intraobserver and interobserver reliability. *Invest Ophthalmol Vis Sci* 1994;**35**:3549–52
65. Urbak SF, Pedersen JK, Thorsen TT. Ultrasound biomicroscopy. II. Intraobserver and interobserver reproducibility of measurements. *Acta Ophthalmol Scand* 1998;**76**:546–9
66. Amaro A, Gangemi R, Piaggio F, Angelini G, Barisione G, Ferrini S, Pfeffer U. The biology of uveal melanoma. *Cancer Metastasis Rev* 2017;**36**:109–40
67. Daniels AB, Veverka KK, Patel SN, Sculley L, Munn G, Pulido JS. Computing uveal melanoma basal diameters: a comparative analysis of several novel techniques with improved accuracy. *Int J Retina Vitreous* 2019;**5**:2
68. Bayat M, Alizad A, Tamminga R, Pulido JS, Fatemi M. Imaging errors in localization of COMS-type plaques in choroidal melanoma brachytherapy. *Invest Ophthalmol Vis Sci* 2013;**54**:6852–60
69. Guthoff RF, Labriola LT, Stachs O. Diagnostic ophthalmic ultrasound. In: Ryan SJ, Sadda SR (eds) *Ryan's retinal imaging and diagnostics*, 2013, pp. e228–85.